

The Proper Motion of PSR J0205+6449 in 3C 58

M. F. Bietenholz^{1,2}, V. Kondratiev^{3,4}, S. Ransom⁵, P. Slane⁶, N. Bartel², and S. Buchner¹

¹*Hartebeesthoek Radio Observatory, PO Box 443, Krugersdorp, 1740, South Africa*

²*Department of Physics and Astronomy, York University, Toronto, M3J 1P3, Ontario, Canada*

³*ASTRON, the Netherlands Institute for Radio Astronomy, Postbus 2, 7990 AA Dwingeloo, The Netherlands*

⁴*Astro Space Center of the Lebedev Physical Institute, Profsoyuznaya str. 84/32, Moscow 117997, Russia*

⁵*National Radio Astronomy Observatory, Charlottesville, VA 22903, USA*

⁶*Harvard-Smithsonian Center for Astrophysics, Theory Division, 60 Garden Street, Cambridge, MA 02138, US*

Accepted for publication on MNRAS; 25 February 2013

ABSTRACT

We report on sensitive phase-referenced and gated 1.4-GHz VLBI radio observations of the pulsar PSR J0205+6449 in the young pulsar-wind nebula 3C 58, made in 2007 and 2010. We employed a novel technique where the ~ 105 -m Green Bank telescope is used simultaneously to obtain single-dish data used to determine the pulsar's period as well as to obtain the VLBI data, allowing the VLBI correlation to be gated synchronously with the pulse to increase the signal-to-noise. The high timing noise of this young pulsar precludes the determination of the proper motion from the pulsar timing. We derive the position of the pulsar accurate at the milliarcsecond level, which is consistent with a re-determined position from the *Chandra* X-ray observations. We reject the original tentative optical identification of the pulsar by Shearer & Neustroev (2008), but rather identify a different optical counterpart on their images, with *R*-band magnitude ~ 24 . We also determine an accurate proper motion for PSR J0205+6449 of (2.3 ± 0.3) mas yr⁻¹, corresponding to a projected velocity of only (35 ± 6) km s⁻¹ for a distance of 3.2 kpc, at p.a. -38° . This projected velocity is quite low compared to the velocity dispersion of known pulsars of ~ 200 km s⁻¹. Our measured proper motion does not suggest any particular kinematic age for the pulsar.

Key words: ISM: supernovae, supernova remnants, pulsar

1 INTRODUCTION

The supernova remnant 3C 58 (G130.7+3.1) has a filled centre morphology and a flat radio spectrum, and was classified on this basis as being pulsar wind nebula (PWN, also pleion; e.g., Weiler & Panagia 1978) long before a pulsar was seen. The pulsar, PSR J0205+6449, was subsequently detected, first in the X-ray (Murray et al. 2002) and then in the radio (Camilo et al. 2002). It is also one of the approximately 100 pulsars that shows pulsed gamma-ray emission (Abdo et al. 2009).

PSR J0205+6449 and 3C 58 are at a distance, D , of ~ 3.2 kpc (Roberts et al. 1993)¹. They have traditionally been associated with the historical supernova of 1181 AD (SN 1181; Clark & Stephenson 1977; Stephenson & Green

1999), giving them an age of 830 yr and making them one of the youngest known supernova remnants and pulsars. However, recent work has suggested that 3C 58 is likely considerably older. In particular, the measured expansion speeds of both the synchrotron bubble (Bietenholz et al. 2001; Bietenholz 2006) and of the thermal filaments (Fesen 1983; Fesen et al. 1988; van den Bergh 1990; Rudie & Fesen 2007), seem to be considerably lower than expected for an age of ~ 830 yr, suggesting an age of several thousand years, which larger age is also suggested several other arguments (see, e.g., Bietenholz 2006; Chevalier 2005).

PSR J0205+6449 has a spin frequency of ~ 15.2 Hz, with a derivative of $\sim -4.5 \times 10^{-11}$ Hz s⁻¹ (Murray et al. 2002; Camilo et al. 2002; Livingstone et al. 2009a), so the characteristic age of the pulsar is 5400 yr. (We note that if the pulsar had an initial spin frequency of ~ 16.3 Hz, the present spin frequency and spindown rate could be reconciled with an age of 830 yr; however as mentioned, numerous other arguments independent of the characteristic age suggest a considerably larger age). It has a high level of timing noise,

¹ Note that the distance is somewhat uncertain, and somewhat larger value is possible. The pulsar dispersion measure is approximately twice what is expected at the distance of 3.2 kpc (Camilo et al. 2002).

having exhibited two spin-up glitches with fractional magnitudes of $\Delta\nu/\nu = 3.4 \times 10^{-7}$ and 3.8×10^{-6} between MJDs 52276 and 53063 (Livingstone et al. 2009a). The pulse width is ~ 2.5 ms (at 1.4 GHz, Camilo et al. 2002). Although as mentioned, there is some controversy over the age of 3C 58, PSR J0205+6449 is nonetheless one of the youngest known pulsars².

PSR J0205+6449 is a particularly interesting case because of the presence of the easily observable pulsar wind nebula, 3C 58. Such nebulae, seen for only a handful of pulsars, provide important diagnostics for young pulsars, giving insight into the winds which carry away the pulsar spindown energies.

Knowing PSR J0205+6449's proper motion is important for determining its exact birthplace as well as the nature of its interaction with its surrounding PWN. More generally, the origin of the high space velocities of pulsars is an interesting question, and therefore knowledge of PSR J0205+6449's proper motion is particularly important because of its young age.

2 PULSAR TIMING WITH GBT: OBSERVATIONS AND RESULTS

We obtained two sessions of pulsar timing observations at the ~ 105 -m diameter Green Bank Robert C. Byrd telescope at Green Bank (GBT), which were carried out simultaneously with the VLBI sessions. We used a new observing technique where the data from the GBT was simultaneously used for both pulsar timing and the VLBI observations. The VLBI data are described in the next session.

On 2007 Apr 25, we observed PSR J0205+6449 with the GBT Spigot back-end (Kaplan et al. 2005) for a duration of 10.8 hrs. The Spigot measures 3-level autocorrelations from each of 2 polarisations for 1024 lags and integrates them for $81.92 \mu\text{s}$ before summing them and writing them to disk. The total bandwidth covered 800 MHz, centred at 1650 MHz, approximately 500 MHz of which (from $\sim 1350 - 1850$ MHz) were free enough from interference to be used for the timing analysis. We let the Spigot continue to take data while the GBT occasionally moved to and from a calibrator source as part of the VLBI scheduling (see below). For these times, which corresponded to about 35% of the total duration, we simply zero-weighted the resulting data from the pulsar. A standard pulsar timing analysis using TEMPO provided us with a pulsar spin ephemeris which we used for pulsar gating of the interferometric data during correlation. We measured a barycentric pulsar spin period of $0.0657176116(4)$ s at epoch MJD 54215.3220 (UTC).

We performed a very similar observation with the newer pulsar back-end GUPPI (Ransom et al. 2009) on 2010 Oct 18, where we observed PSR J0205+6449 for 8.9 hrs. GUPPI recorded the 8-bit, summed polarisations from 2048 channels every $192 \mu\text{s}$ covering 800 MHz of bandwidth (of which the highest ~ 600 MHz was usable). After zero-weighting data when the GBT was off of the pulsar's position, a timing

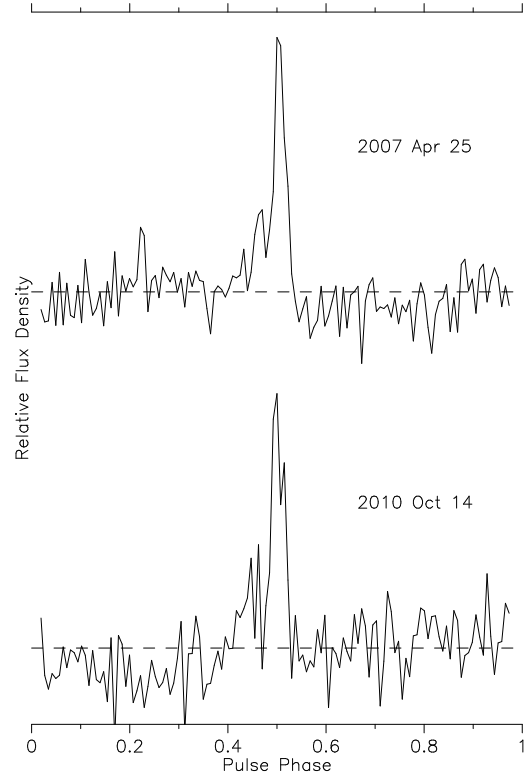


Figure 1. Pulse profiles obtained with GBT at our two observing epochs. The profiles have 128 bins, and have been shifted so that the peaks occur at phase = 0.5, and the zero-level in each profile is indicated by the dashed horizontal line. We do not consider the differences between the two profiles significant.

analysis determined the barycentric pulsar spin period to be $0.0657388555(6)$ s at epoch MJD 55487.8302 (UTC).

For our timing analyses we used a simple two-Gaussian model as our template profile where the peak of the pulsar flux occurred very near to spin phase 0.5. We assumed a pulsar position, dispersion measure, and instantaneous spin-down rates consistent with those measured by Livingstone et al. (2009b).

We show the average pulse profiles obtained in the two observing sessions in Figure 1. As the pulsar is quite weak, the signal-to-noise ratio is relatively low, and consequently we do not consider the differences between the two profiles significant. The FWHM duty-cycle the pulse is $\sim 6\%$.

3 VLBI RADIO OBSERVATIONS

We obtained two epochs of 1.4-GHz VLBI observations of PSR J0205+6449 using the “High Sensitivity Array”, which consisted of the NRAO Very Long Baseline Array (VLBA) augmented by the GBT (~ 105 m diameter) and Effelsberg (100 m diameter) telescopes. For the first session, on 2007 April 25 (program code BB241), we obtained 10 hours of VLBI data, while for the second session on 2010 October 18 (program code BB295), we obtained 12 hours. In each session we recorded both senses of circular polarisation, and we used 2-bit sampling at a bit rate of 512 Mbit s^{-1} , for an effective bandwidth per polarisation of 64 MHz.

The data from 2007 were correlated with NRAO's

² Several pulsars or PWNe, including the Crab Nebula, G21.5–0.9 (Bietenholz & Bartel 2008) and Kes 75 (Gotthelf et al. 2000) are thought to be only around 1000 yr old, but the vast majority of known pulsars have ages $> 10,000$ yr.

VLBA processor, while those from 2010 were correlated with the DiFX processor (Deller et al. 2011). The analysis was carried out with NRAO’s Astronomical Image Processing System (AIPS). During correlation, we gated the correlator using the pulsar timing extracted from the GBT data, and accumulated several sets of VLBI data with different gating: firstly, the un-gated data, and secondly, the “on-pulse” gated data where the gated bin had a width of 8% of the pulsar period (distributed symmetrically about the peak). In addition, for the 2010 data, correlated with the DiFX correlator, we also accumulated data in 12 different bins evenly distributed in pulse phase, with each bin therefore having a width of 8.33% of the period. In all data sets we used a correlator integration time of 3.0 s.

We used VCS2 J0209+6437 (Fomalont et al. 2003), 0.5° away from PSR J0205+6449, as our primary phase-reference source, but we included some observations of an astrometric check source, JVAS J0228+6721(4C 67.05, ICRF J022850.0+672103; IERS B0224+671), which is a source in the International Celestial Reference Frame catalogue whose position is accurately known (Fey et al. 2009), and which is 3.4° away from PSR J0205+6449. For the phase-centre position for the pulsar observations, we use the position of the pulsar given in Slane et al. (2002), $02^{\text{h}} 05^{\text{m}} 37^{\text{s}}.92$, $64^\circ 49' 42''.8$. Mostly we used a cycle time of 3.8 minutes, with 2.5 minutes being spent on PSR J0205+6449. The calibration of the VLBI data was done using standard procedures using NRAO’s AIPS package. The flux density calibration was done through measurements of the system temperature at each telescope, and the antenna amplitude gains were subsequently improved through self-calibration of the reference sources.

Some sporadic radio-frequency interference (RFI) was seen, particularly in the frequency range 1617 to 1625 MHz. We clipped out visibility points with anomalously high amplitudes, removing $\lesssim 1\%$ of the data. We also deleted any data taken when either of the antennas were at elevations of $< 10^\circ$. During our 2007 observing run, the GBT failed to observe J0209+6437 for three periods of approximately one hour. We discarded all the GBT data for all sources from these periods.

The fringe-fitting and phase calibration was done using the (un-gated) data from our calibrator sources. We estimated the ionospheric delay using the AIPS task TECOR using IONEX data from the Crustal Dynamics Data Information System archive³ of the Goddard Space Flight Center. The earth orientation parameters used during the correlation were extrapolated. We corrected to more accurate ones subsequently made available from the United States Naval Observatory. The resulting calibration was then interpolated to the times of the PSR J0205+6449 as well as the J0228+6721 observations, and applied to both the gated and un-gated visibility data for PSR J0205+6449.

3.1 Astrometric Reference Sources

Our primary phase-reference source was J0209+6437. We take, as the astrometric reference point for J0209+6437, the peak brightness position, for which we take the coordinates

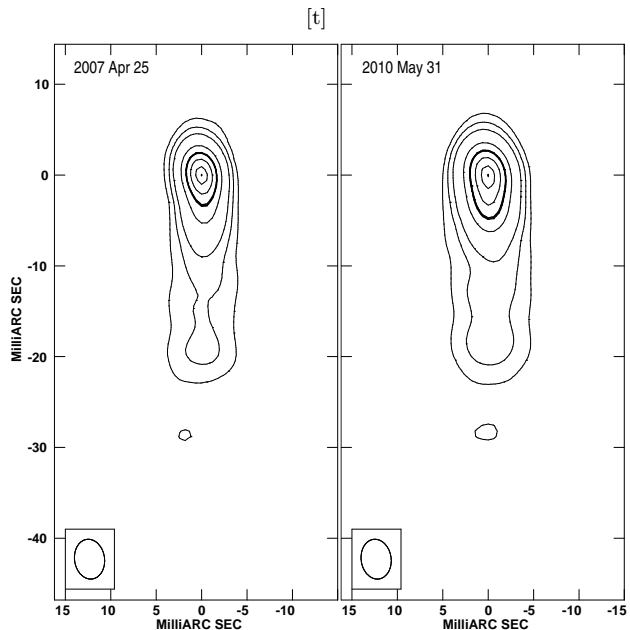


Figure 2. VLBI images of J0209+6437 on our two observing epochs. The contours are drawn at 2, 5, 10, 30, **50**, 70, 90 and 99% of the peak brightness, with the 50% contour being emphasized. The two images have been convolved with the same restoring beam of $\text{FWHM } 4.4 \times 3.3 \text{ mas}$ at p.a. 8° indicated at lower left. The peak brightness was 81 and 59 $\text{mJy } \text{bm}^{-1}$ for 2007 and 2010, respectively. In each panel, the origin is placed at the peak-brightness point, which we use as the astrometric reference point.

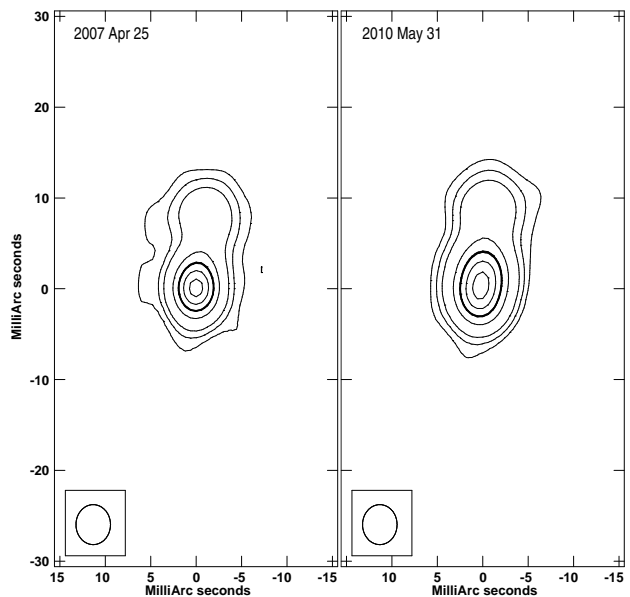


Figure 3. VLBI images of J0228+6721 on our two observing epochs. The contours are drawn at 2, 5, 10, 30, **50**, 70, 90 and 99% of the peak brightness, with the 50% contour being emphasized. The two images have been convolved with the same restoring beam of $\text{FWHM } 4.4 \times 3.8 \text{ mas}$ at p.a. 0° indicated at lower left. The peak brightness was 601 and 421 $\text{mJy } \text{bm}^{-1}$ for 2007 and 2010, respectively. The visibility data were self-calibrated in phase before imaging to best show the intrinsic structure.

³ <http://cddis.gsfc.nasa.gov>

02^h 09^m 35^s.98806(20), 64° 37' 25".7701(06) from the VCS2 Survey (Fomalont et al. 2003), where the numbers in parentheses give the uncertainty in the last two digits. Unfortunately, this source turned out to be somewhat resolved. We show the VLBI images of J0209+6437 on our two observing epochs in Figure 2. The source is elongated in the north-south direction, with the 50% contour having an extent of approximately 6 mas.

It is possible that the peak brightness position, and therefore our astrometric reference point, varies with time due to changes in the source morphology (see, e.g., Bietenholz et al. 2000; Bartel et al. 2012)

As mentioned, we also included some observations of an astrometric check source, J0228+6721. Like our observations of PSR J0205+6449, we phase-reference our observations of J0228+6721 to J0209+6437. We give the peak brightness positions of J0228+6721, as well as the ICRF position in Table 1.

Unfortunately, this source is also extended at the mas level in the N-S direction (Lister et al. 2009a; Romney et al. 1984; Perley et al. 1980). Moreover, this source is known to have a somewhat variable morphology (Lister et al. 2009b; Bondi et al. 1996; Padrielli et al. 1986), with both changes in the size of the central component, and motions of other components being observed with magnitudes of up to $\sim 0.3 \text{ mas yr}^{-1}$. We show images of J0228+6721 in Figure 3.

3.2 PSR J0205+6449

The pulsar was expected to be quite faint: even in the images made from gated VLBI data, we expected a signal-to-noise ratio of $\lesssim 10$. Furthermore, the pulsar position is not accurately known *a priori*. In order not to bias our analysis by searching only near an assumed position, we therefore chose to image a fairly large region. We imaged PSR J0205+6449 directly from the calibrated multi-channel VLBI data without any averaging of the visibility data in frequency. Since our channel width was 0.5 MHz, the field of view over which bandwidth smearing is small is $> 10''$, which is adequate for our purposes. We made images of 4096×4096 pixels, with the pixels being $0.8 \times 0.8 \text{ mas}$, centred on our initial position estimate for PSR J0205+6449, which was the position was used in the correlation, and was the one given by Slane et al. (2002) of 02^h 05^m 37^s.92, 64° 49' 42".8 (J2000). Our images therefore span a region $\pm \sim 2''$ from this estimated position, which should be larger than any expected uncertainty in the X-ray derived position. We used natural weighting to obtain the highest signal-to-noise ratio. We evaluated the image rms brightness over the central 90% of the image area, excluding a narrow region around the edge where the rms is typically slightly higher due to gridding artifacts.

In Table 2 we give the signal-to-noise ratios of the brightness extrema in the various images. In the images made from un-gated visibility data, the positive and negative extrema were of similar magnitude, being $\leq 5.5\sigma$ where σ was the image brightness rms. In the images made from the on-pulse gated data, for both epochs, the negative extrema were of a similar magnitude. For both epochs however, the images made from the on-pulse data showed a single positive peak that was $\geq 6.5\sigma$, or larger in magnitude than the negative extremum by $\geq 1\sigma$. The number of independent sky positions sampled by our images can be estimated by divid-

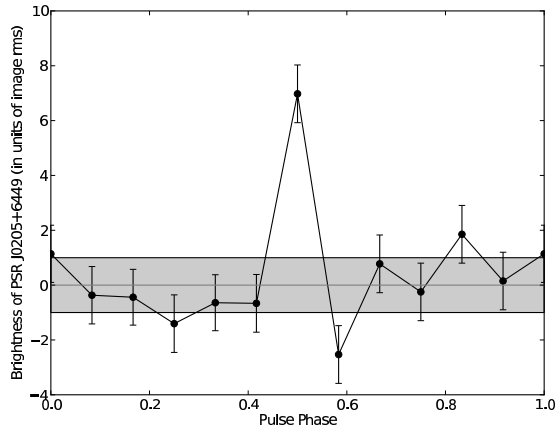


Figure 5. The pulse profile of PSR J0205+6449: the image brightness, given in units of the image rms (σ) at the location of PSR J0205+6449 in the images made from the data in each of 12 bins distributed across the pulsar period. The first bin on the left is duplicated on the right for clarity. The shaded area shows the $\pm 1\sigma$ region. Only in the bin at pulse phase = 0.5 is a signal substantially in excess of the noise visible.

ing the image area by the FWHM area of the fitted beam, and was $\sim 650,000$. If the pixel brightnesses are Gaussian-distributed, the likelihood of obtaining a value in excess of $\pm 6\sigma$ in 650,000 trials is then $\sim 0.1\%$, although we note that the distribution of pixel brightnesses may not be accurately Gaussian at these large deviations from 0.

Furthermore, the two positive extrema seen in the images made from the gated data were quite close to one another on the sky, being within 6 mas of each other on the sky. Since the total area we examined was $\sim 10^7 \text{ mas}^2$, the odds of random peaks occurring so close together would be ~ 80000 to 1 (which probability is independent of the actual distribution of pixel brightnesses).

In Figure 4 we show a section of the images made from the gated on-pulse and un-gated visibility data sets from 2010. Although the signal-to-noise is not high, the pulsar can be clearly seen in the on-pulse image, but not in the corresponding un-gated one.

Despite the modest signal-to-noise ratio, we think that the detections are firm for several reasons. Firstly, in each of the “on-pulse” images, the positive extremum in the image (excluding a ~ 100 -pixel strip around the edge where the rms is somewhat higher due to numerical artifacts) is $\geq 1\sigma$ higher than the corresponding negative one, which is not expected to happen by chance. Secondly, no source is visible in either of the un-gated images at this location. Any background source should be much more strongly detected in the images made from the un-gated data since the gated visibility data represents only $\sim 8\%$ of the total observations.

As an additional check, for the 2010 observations, we imaged separately the visibility data from the 12 bins spaced evenly across the pulsar period. In Figure 5 we show brightness at the location determined from the on-pulse image as a function of the pulse phase. The profile can be compared to that obtained from the GBT pulsar-timing observations shown in Figure 1 above.

We note here that position of PSR J0205+6449 is dif-

Table 1. Position of J0228+6721.

Observations	Frequency (GHz)	RA (J2000)			Decl. (J2000)			Offset(mas) ^a	
		hr	m	s	°	'	"	RA	decl.
ICRF (Fey et al. 2009)	8.4	02	28	50.05148948	67	21	03.0293039		
2007 VLBI obs. ^b	1.4	02	28	50.0516247	67	21	03.033364	0.78	4.06
2010 VLBI obs. ^b	1.4	02	28	50.0516134	67	21	03.035272	0.72	5.97

^aOffset of measured position from the ICRF position.

^bPositions measured from peak-brightness point, and measured relative to J0209+6437, which is assumed to be at the VCS2 position (see text).

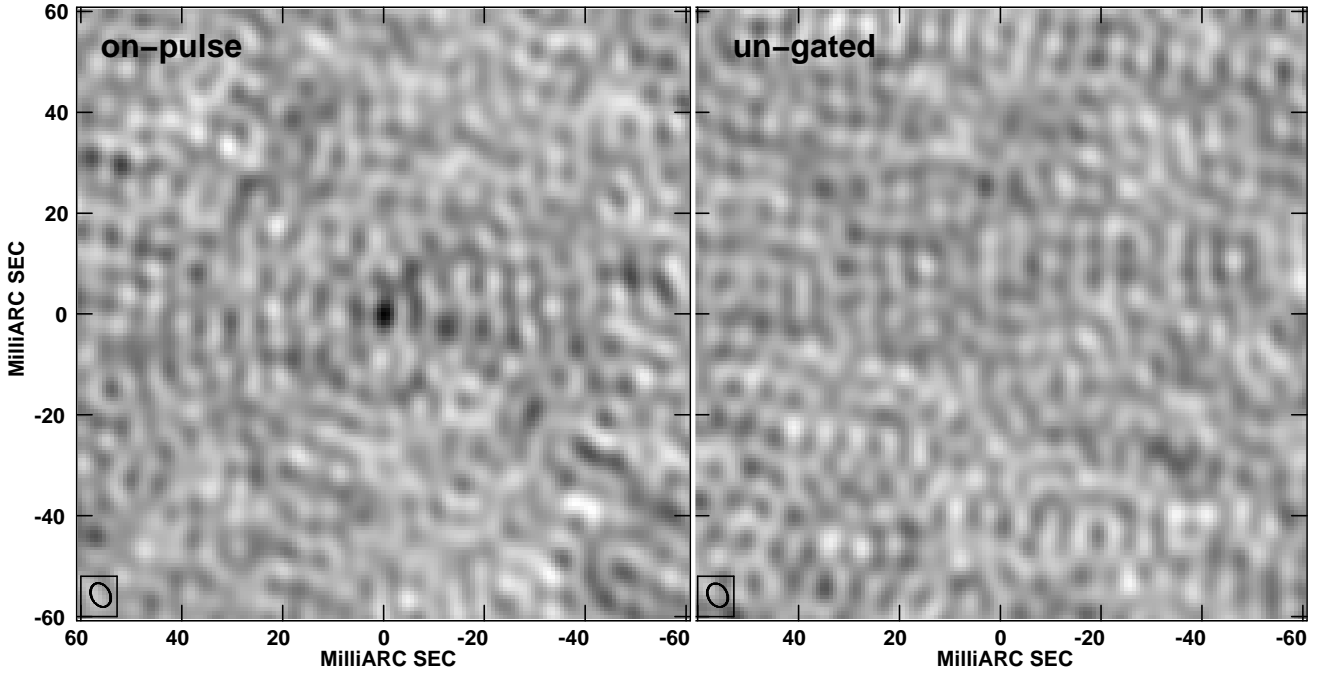


Figure 4. VLBI images of PSR J0205+6449 from our 2007 observations. Both images are dirty or undeconvolved. In both panels, the grey-scale runs from -3.8σ (white) to 6.9σ (black), and the FWHM of an elliptical Gaussian fit central part of the beam is shown at lower left. The left panel shows the image made from the on-pulse gated visibility data, while the right panel shows the image made from the un-gated visibility data. The images are centred on PSR J0205+6449, only visible in the left panel, which is at $02^{\text{h}} 05^{\text{m}} 37^{\text{s}}.92322$, $64^{\circ} 49' 41''.3319$.

Table 2. Position of PSR J0205+6449.

Observation Epoch	Gating	Image Extrema (in units of image rms)		RA (J2000) hr m s	^a	Decl. (J2000) ° ' "	^a
2007	Off-pulse	−5.1	+5.1	(not detected)			
2007	On-pulse	−5.0	+6.8	02 05 37.92322	(1)	64 49 41.3319	(4)
2010	Off-pulse	−5.5	+5.2	(not detected)			
2010	On-pulse	−5.1	+6.5	02 05 37.92247	(1)	64 49 41.3343	(4)

^a The position of the brightness peak of PSR J0205+6449. The digit in parentheses gives the statistical uncertainty in the last digit of the corresponding coordinate value; note that the total uncertainty is dominated by a systematic component discussed in the text.

ferent than that of the point source visible in the X-ray as given in Slane et al. (2002) of $02^{\text{h}} 05^{\text{m}} 37^{\text{s}}.92$, $64^{\circ} 49' 42''.8$ by $\sim 1''.5$.

3.3 Proper Motion of PSR J0205+6449

Using the position determinations in Table 2 we obtained the displacement of PSR J0205+6449 between our two observing epochs to be -4800 ± 570 , $+2800 \pm 570$ μas in RA and Decl., respectively, where the uncertainties are statistical only. At a distance of 3.2 kpc, the parallax of PSR J0205+6449 is expected to be 313 μas , smaller than the statistical uncertainty, but as the angular displacement due to parallax is readily calculable we corrected for it. The expected shift between our two particular epochs due to parallax is to be 36 and 499 μas in RA and Decl., respectively. Correcting for the parallax, we then arrive at a net displacement of PSR J0205+6449 between our two epochs of -4860 ± 570 , $+2330 \pm 570$ μas in RA and Decl., respectively (where we have ignored the small additional uncertainty incurred due to the uncertainty in the distance). This displacement corresponds to a proper motion of -1400 ± 160 $\mu\text{as yr}^{-1}$ in RA and 540 ± 160 $\mu\text{as yr}^{-1}$ in Decl., or 1500 ± 160 $\mu\text{as yr}^{-1}$ at p.a. $159 \pm 6^{\circ}$, where the proper motion is measured relative to the brightness peak of J0209+6437, and the uncertainties are statistical only.

Since our reference source, J0209+6437, is somewhat resolved, we must carefully assess any possible effect of temporal changes in J0209+6437 on our proper motion measurements. In our VLBI observations, we observed a check source, J0228+6721 in a fashion similar to PSR J0205+6449, in particular similarly phase-referenced to J0209+6437. The positions measured for the check source were given in Table 1, and suggest a proper motion for J0228+6721 of -1 and 550 $\mu\text{as yr}^{-1}$ in RA and Decl., respectively. The source J0228+6721 is an ICRF source and Feissel-Vernier (2003) finds a proper motion of < 50 $\mu\text{as yr}^{-1}$ at 8.4 GHz over a period of ~ 12 years. However, the lack of secular motions at 8.4 GHz, where the core is likely more dominant, does not preclude apparent motions at our lower frequency of 1.4 GHz, where jet components are more likely to dominate the emission. Indeed, other authors have reported larger proper motions for components within J0228+6721: Bondi et al. (1996) find an expansion of 300 $\mu\text{as yr}^{-1}$ while Lister et al. (2009b) find several moving components with proper motions of up to 376 $\mu\text{as yr}^{-1}$ at 14 GHz. It is therefore possible that our observed proper motion is due to component motions within J0228+6721. It is, however, also possible that our primary reference source, J0209+6437, is not in fact stable. Unfortunately, both our reference sources are elongated in the north-south direction, so that the observed north-south relative motion between them could be the result of motions along the jet axis in either source.

As a conservative estimate of 1σ uncertainty on the proper motion of PSR J0205+6449, as phase-referenced to J0209+6437, we therefore take the apparent proper motion of J0228+6721 found above. We then arrive at a final value for the proper motion of PSR J0205+6449 of -1400 ± 160 $\mu\text{as yr}^{-1}$ in RA and 540 ± 575 $\mu\text{as yr}^{-1}$ in Decl. At a distance of 3.2 kpc, this corresponds to a speed of 23 ± 6 km s^{-1} . Note, however, that this velocity is with respect to the Earth. We calculate a more physical value of

PSR J0205+6449's projected velocity, corrected for Galactic rotation and the Sun's motion, in § 5 below.

4 X RAY ASTROMETRY

To determine the X-ray position of PSR J0205+6449, we investigated data from a deep *Chandra* observation carried out between 2003 April 22 and 26 (see Slane et al. 2004, for details and original results from these observations). The data from observation IDs 4383, 4382, and 3832 were reprocessed and cleaned using standard routines from *Ciao* version 4.4. The `merge.all` task was used to create a merged image from the 317 ks of good exposure time. The pulsar is embedded in a bright compact nebula that is slightly asymmetric in the east-west direction. The centroid of the point source emission is located at a position of $02^{\text{h}} 05^{\text{m}} 37^{\text{s}}.93$, $+64^{\circ} 49' 41.4''$. We identified three X-ray point sources in the field that have counterparts in the 2MASS catalogue. Comparing the centroid positions of the X-ray sources with the infrared positions, we find that the uncertainty in the *Chandra* position of the pulsar is $\sigma_{\text{RA}} \sim 0.06$ s and $\sigma_{\text{dec}} \sim 0.12''$. The systematic error associated with contributions from the compact nebula are estimated to be slightly larger than these values, but the combined uncertainty is $\lesssim 1$ arcsecond either direction.

We note that position given above is slightly different from that determined in the shorter *Chandra* observation reported by Slane et al. (2002). We have reprocessed those earlier data (observation ID 728) as well, and find that the position is in excellent agreement with the value given above. We conclude that there were small errors in the initial position reconstructions reported by Slane et al. (2002).

5 DISCUSSION

Using gated VLBI we imaged PSR J0205+6449 in the centre of 3C 58. The pulsar was detected. The position of PSR J0205+6449 we found from the VLBI observations was $\sim 1''.5$ distant from the originally published one of a compact X-ray source seen in *Chandra* ACIS observations (Slane et al. 2002). A re-examination of the *Chandra* data, however, resulted in an improved position of the X-ray source which is well within the uncertainties of that measured with VLBI.

Shearer & Neustroev (2008) report of deep optical observations of the centre of 3C 58 using the 4.2 m William Herschel Telescope in La Palma, in which they detect three unresolved sources with *R*-band magnitudes of ~ 24 , in addition to the more diffuse synchrotron emission from the pulsar wind nebula. Shearer & Neustroev (2008) tentatively identified their source “o1” as PSR J0205+6449 on the basis of its coincidence with the published position of the compact X-ray source. However, based on our VLBI determination and the re-determined *Chandra* HRC position, it is in fact their object “o2”, which is almost certainly the optical counterpart of PSR J0205+6449. The position of o2 is RA = $02^{\text{h}} 05^{\text{m}} 37^{\text{s}}.93$ and Decl. = $64^{\circ} 49' 41''.4$, with an uncertainty of $\lesssim 0''.1$, consistent to within $0''.08$ with the pulsar position determined from VLBI. Shearer & Neustroev (2008) give the magnitudes of o2 as 24.15 ± 0.07 in *R*, > 24.3 in *V* and < 25.6 in *B*, consistent with the optical magnitudes estimated for

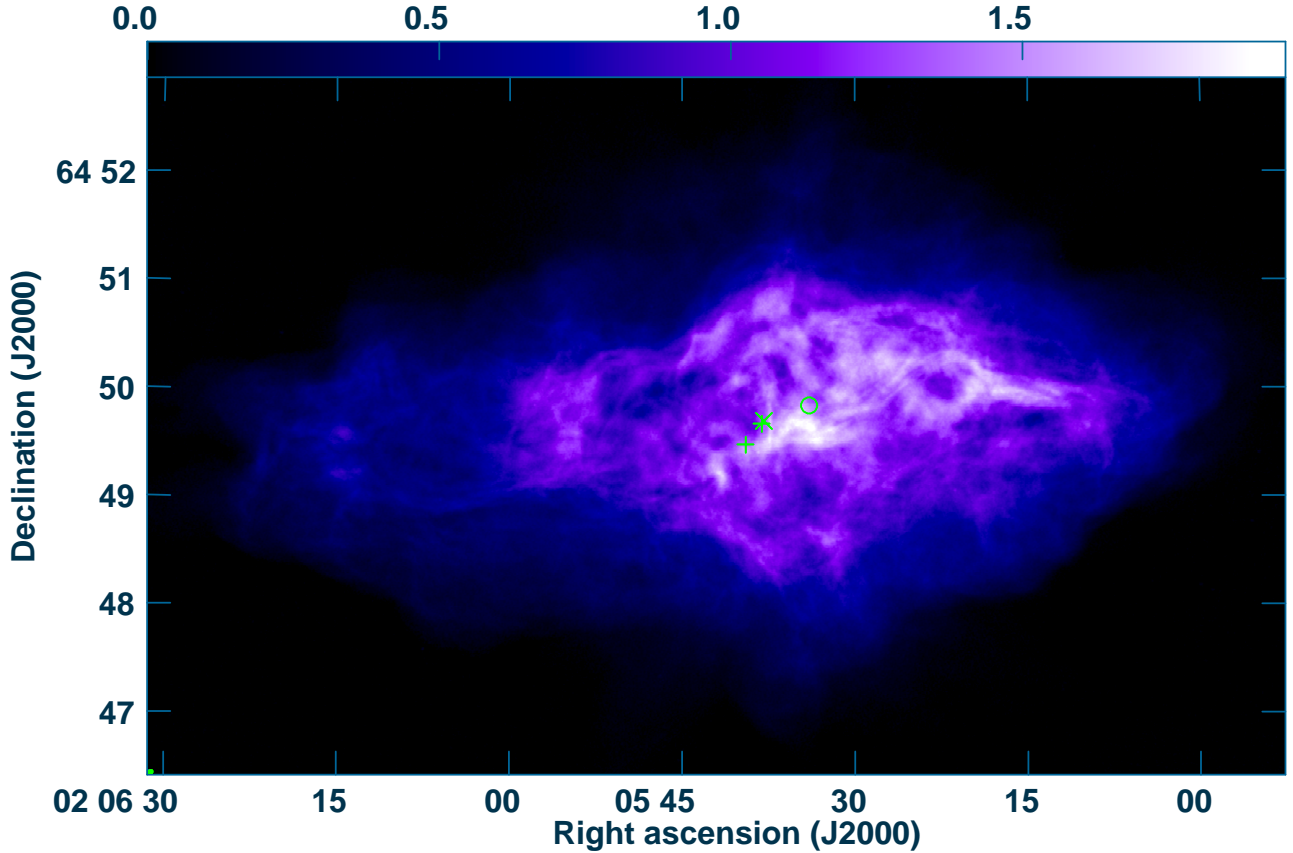


Figure 6. A 1.4-GHz VLA radio image of 3C 58, reproduced from Bietenholz (2006). The “x” sign shows the present location of PSR J0205+6449, while the two “+” signs show the extrapolated position at two possible dates of the supernova explosion which gave rise to 3C 58: at 1181 AD and at 5000 BC, with the one at 1181 AD being the one overlapping with the present position (x). The “o” shows the position of the centre of the circular region of softer X-ray emission, interpreted as thermal emission from the supernova shell, from Gotthelf et al. (2007). The grey-scale is labelled in mJy bm^{-1} , and the FWHM resolution was $1''.4$. We show a detail of the central region in Fig. 7 below.

PSR J0205+6449 based on its spindown luminosity, distance and the expected Galactic extinction.

In summary, we can regard the detection of PSR J0205+6449 in the radio, optical and X-ray bands as firm, with the most accurate position being that determined from the VLBI observations and given in Table 2 above.

In addition to determining the position, we also determined the proper motion of PSR J0205+6449 of $-1400 \pm 160 \mu\text{as yr}^{-1}$ in RA and $670 \pm 575 \mu\text{as yr}^{-1}$ in Decl. In order to correct this measured value for Galactic rotation and the Earth’s motion with respect to the local standard of rest, we take the Galactic constants from Schönrich (2012), namely a flat Galactic rotation curve with $v = 238 \text{ km s}^{-1}$ and a distance to the Galactic centre of 8.27 kpc. We take also from Schönrich (2012) the Solar motion of 250 km s^{-1} in the Galactic plane, solar radial velocity of 14 km s^{-1} towards the Galactic centre, and a motion of 6.1 km s^{-1} perpendicular to the Galactic plane. We take the distance of PSR J0205+6449 (from Earth) to be 3.2 kpc. We can then calculate the peculiar motion of PSR J0205+6449 with respect to the standard of rest at its location as being⁴ $2.3 \pm 0.3 \text{ mas yr}^{-1}$, corre-

sponding to $35 \pm 6 \text{ km s}^{-1}$ at p.a. -38° (p.a. in equatorial rather than Galactic frame).

This speed is relatively small: Galactic pulsars have a 2-D velocity dispersion of $200 \sim 300 \text{ km s}^{-1}$ (e.g., Hobbs et al. 2005; Lyne & Graham-Smith 1990). Even taking the uncertainty introduced by possible motion of our reference source, the 3σ upper limit on the proper motion of PSR J0205+6449 is only 53 km s^{-1} .

Can PSR J0205+6449’s low tangential velocity be reconciled with the velocity distribution of other Galactic pulsars? Faucher-Giguère & Kaspi (2006) found that the distribution of space velocities of Galactic pulsars at birth was consistent with one where each of the three orthogonal components of the space velocity was distributed exponentially, with the mean of the absolute value of each component being $180^{+20}_{-30} \text{ km s}^{-1}$, and the resulting mean three-dimensional speed being $380^{+40}_{-60} \text{ km s}^{-1}$. Since PSR J0205+6449 is quite young (we discuss the age in more detail below), its velocity is probably close to its birth velocity. As the multi-dimensional exponential distribution of Faucher-Giguère &

⁴ We noted above that the proper motion uncertainty is rather

larger in Decl. than in RA. Here we take the geometric mean of the two values.

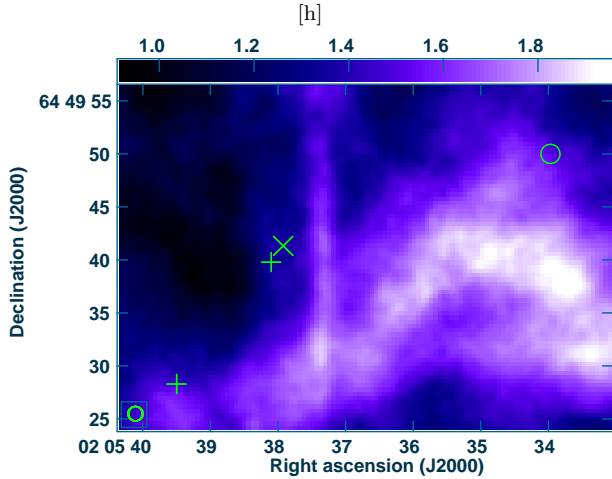


Figure 7. Detail of the 1.4 GHz VLA radio image of 3C 58 from Figure 6 above. The symbols have the same meanings as in that figure. The restoring beam FWHM of $1''.4$ is indicated by the circle in the lower left corner.

Kaspi (2006) is difficult to evaluate numerically, we performed a Monte-Carlo simulation with $n = 10000$ trials, to find that the chance of finding a pulsar with a tangential velocity as small as the $35 \pm 6 \text{ km s}^{-1}$ measured for PSR J0205+6449 from such a distribution is $\sim 2.7\%$.

Alternatively, Hobbs et al. (2005) collected proper motion measurements for 140 pulsars⁵. Of their sample, 8, or 5.7% had tangential velocities $\leq 35 \text{ km s}^{-1}$. Finally, some authors have found the distribution of pulsar velocities to be bi-modal. For example, Briskin et al. (2003) find that 20% of pulsars form a low-velocity component with a one-dimensional velocity dispersion, σ_{v1D} of 99 km s^{-1} , while the remainder have a $\sigma_{v1D} = 294 \text{ km s}^{-1}$. In this case, the probability of a random pulsar having a tangential velocity as low as 35 km s^{-1} is 1.8%.

In conclusion, the small measured proper motion makes PSR J0205+6449 somewhat unusual in being amongst the slowest few percent of young pulsars regardless of whether a bimodal or a unimodal distribution of pulsar velocities is considered.

Our estimate of the tangential velocity depends on the distance to PSR J0205+6449 and 3C 58, which, as mentioned earlier, is somewhat uncertain. The value of 3.2 kpc of Roberts et al. (1993) was determined kinematically from HI absorption. Kothes (2010) argues for a distance of ~ 2 kpc. Adopting a smaller distance would reduce the tangential velocity estimate by the corresponding factor, and thus make PSR J0205+6449's low speed even more unlikely. The low measured angular speed therefore argues against a distance much lower than 3.2 kpc.

On the other hand, PSR J0205+6449's dispersion measure is approximately twice that expected for a distance of 3.2 kpc (Camilo et al. 2002), suggesting perhaps that the true distance is somewhat larger, which would imply a

tangential velocity larger by a factor of $(D/3.2 \text{ kpc})$. This question could be resolved with a measurement of PSR J0205+6449's trigonometric parallax with 10% accuracy. Such a measurement is feasible if an in-beam calibrator can be found (see e.g., Chatterjee et al. 2009), and should be undertaken.

Can we extrapolate back from PSR J0205+6449's present position to determine its position at the time of the supernova explosion? To do so requires knowing the age of PSR J0205+6449. As noted in the introduction, although it has traditionally been associated with a supernova in 1181 AD, making it ~ 830 yr old, it is probably older, with a likely age of ~ 7000 yr (Bietenholz 2006; Bietenholz et al. 2001), suggesting an epoch of ~ 5000 BC for the supernova event. In Figure 6 we show a radio image of 3C 58, and indicate the present, and extrapolated epoch 1181 AD and 5000 BC positions of PSR J0205+6449.

From *XMM-Newton* X-ray observations of 3C 58, Gotthelf et al. (2007; see also Bocchino et al. 2001) found an approximately circular region with a softer X-ray spectrum, which they interpreted as a thermal X-ray emission from the supernova shell. They noted, however, that the centre of this shell was displaced from the pulsar position at $02^{\text{h}} 05^{\text{m}} 33^{\text{s}}.97, 63^{\circ} 49' 50''.0$ (J2000.0). We plot this position also in Figure 6. Neither the present distribution of synchrotron emission or thermal filaments suggests any particular explosion centre, and although Fesen et al. (2008) determined proper motions for various optical features, the precision is too low to accurately identify an expansion centre.

Our measured proper motion does not place PSR J0205+6449 near the centre of the region of softer X-ray emission for either possible explosion epoch. For an explosion epoch of 5000 BC, however, the extrapolated position of PSR J0205+6449 is closer to the geometrical centre of 3C 58.

If the area of softer X-ray emission identified by Gotthelf et al. (2007) were thermal X-ray emission associated with the forward shock of the supernova, then one would probably expect its centre to be near the location of the explosion and of PSR J0205+6449's birth. This does not seem to be the case. Furthermore, the diameter of the region of softer X-ray emission is only ~ 5.6 pc, which is notably smaller than the PWN, which has an E-W extent of ~ 8.5 pc. The PWN, however, is expected to still be confined by the ejecta and thus be inside the forward shock, which suggests that the forward shock is considerably larger than the region of softer X-ray emission. Therefore, both because the region of softer X-ray emission is not centred on the location of the explosion, and because it is small compared to the PWN, we think it is unlikely that the softer X-ray emission is associated with the supernova forward shock.

6 SUMMARY AND CONCLUSION

1. We obtained VLBI observations of PSR J0205+6449, the pulsar in 3C 58. We employed a novel technique to obtain VLBI observations of faint pulsars, where we used the GBT simultaneously for pulsar timing observations as well as an element of the VLBI array. The derived pulsar timing information was then used to gate the VLBI correlator increasing

⁵ In fact, Hobbs et al. (2005) collected proper motion measurements of 175 pulsars, but we exclude the 35 recycled pulsars from Hobbs' sample as they are much older and have a notably lower velocity dispersion than the remainder.

the signal-to-noise of the pulsar VLBI. This technique can be used to advantage for other young pulsars which have high timing noise.

2. We determined an accurate position for PSR J0205+6449 of $02^{\text{h}} 05^{\text{m}} 37^{\text{s}}.92 \ 64^{\circ} 49' 41''.3$, which is $1''.5$ different than the previously accepted one, which was based on an X-ray image. Re-examination of the X-ray data, however, reveal an error in the original reported position; the newly-determined X-ray position reported here is consistent with the VLBI position. Furthermore, this position is coincident with an optical source identified by Shearer & Neustroev (2008).

3. We determined the proper motion of PSR J0205+6449. After correction for Galactic rotation, we found a proper motion of $2.3 \pm 0.3 \text{ mas yr}^{-1}$, corresponding to tangential velocity of $(35 \pm 6)(D/3.2 \text{ kpc}) \text{ km s}^{-1}$ at p.a. -38° . This low speed puts PSR J0205+6449 amongst the slowest few percent of young pulsars.

4. We estimated PSR J0205+6449's position at birth. If it is the remnant of a supernova in 1181 AD, then its position at birth is only $1''.9$ different than at present. If as seems more likely, the age of PSR J0205+6449 and 3C 58 is several thousand years, then its position at birth was near the midpoint of the presently visible nebula, although somewhat displaced from the present radio brightness centre which is close to the present location of PSR J0205+6449.

ACKNOWLEDGEMENTS

The research at York University was supported by the National Sciences and Engineering Research Council of Canada. POS acknowledges partial support from NASA contract NAS8-03060. The National Radio Astronomy Observatory, NRAO, is a facility of the National Science Foundation operated under cooperative agreement by Associated Universities, Inc. The telescope at Effelsberg is operated by the Max-Planck-Institut für Radioastronomie in Bonn, Germany. This publication makes use of data products from the Two Micron All Sky Survey, which is a joint project of the University of Massachusetts and the Infrared Processing and Analysis Center/California Institute of Technology, funded by the National Aeronautics and Space Administration and the National Science Foundation. We have made use of NASA's Astrophysics Data System Bibliographic Services.

REFERENCES

- Abdo A. A. et al., 2009, *ApJL*, 699, L102
 Bartel N., Bietenholz M. F., Lebach D. E., Lederman J. I., Petrov L., Ransom R. R., Ratner M. I., Shapiro I. I., 2012, *ApJS*, 201, 3
 Bietenholz M. F., 2006, *ApJ*, 645, 1180
 Bietenholz M. F., Bartel N., 2008, *MNRAS*, 386, 1411
 Bietenholz M. F., Bartel N., Rupen M. P., 2000, *ApJ*, 532, 895
 Bietenholz M. F., Kassim N. E., Weiler K. W., 2001, *ApJ*, 560, 772
 Bocchino F., Warwick R. S., Marty P., Lumb D., Becker W., Pigot C., 2001, *Astron. Astrophys.*, 369, 1078
 Bondi M. et al., 1996, *Astron. Astrophys.*, 308, 415
 Briskin W. F., Fruchter A. S., Goss W. M., Herrnstein R. M., Thorsett S. E., 2003, *AJ*, 126, 3090
 Camilo F. et al., 2002, *ApJL*, 571, L41
 Chatterjee S. et al., 2009, *ApJ*, 698, 250
 Chevalier R. A., 2005, *ApJ*, 619, 839
 Clark D. H., Stephenson F. R., 1977, *The historical supernovae*. Oxford [Eng.] ; New York : Pergamon Press, 1977. 1st ed.
 Deller A. T. et al., 2011, *PASP*, 123, 275
 Faucher-Giguère C.-A., Kaspi V. M., 2006, *ApJ*, 643, 332
 Feissel-Vernier M., 2003, *Astron. Astrophys.*, 403, 105
 Fesen R., Rudie G., Hurford A., Soto A., 2008, *ApJS*, 174, 379
 Fesen R. A., 1983, *ApJL*, 270, L53
 Fesen R. A., Kirshner R. P., Becker R. H., 1988, in *IAU Colloq. 101: Supernova Remnants and the Interstellar Medium*, p. 55
 Fey A. L., Gordon D., Jacobs C. S., eds., 2009, *IERS Technical Note, Vol. 35, The Second Realization of the International Celestial Reference Frame by Very Long Baseline Interferometry*. Frankfurt: Verlag des Bundesamts für Kartographie und Geodäsie, p. 1
 Fomalont E. B., Petrov L., MacMillan D. S., Gordon D., Ma C., 2003, *AJ*, 126, 2562
 Gotthelf E. V., Helfand D. J., Newburgh L., 2007, *ApJ*, 654, 267
 Gotthelf E. V., Vasisht G., Boylan-Kolchin M., Torii K., 2000, *ApJL*, 542, L37
 Hobbs G., Lorimer D. R., Lyne A. G., Kramer M., 2005, *MNRAS*, 360, 974
 Kaplan D. L. et al., 2005, *PASP*, 117, 643
 Kothes R., 2010, in *Astronomical Society of the Pacific Conference Series, Vol. 438, Astronomical Society of the Pacific Conference Series*, R. Kothes, T. L. Landecker, & A. G. Willis, ed., p. 347
 Lister M. L. et al., 2009a, *AJ*, 137, 3718
 Lister M. L. et al., 2009b, *AJ*, 138, 1874
 Livingstone M. A., Ransom S. M., Camilo F., Kaspi V. M., Lyne A. G., Kramer M., Stairs I. H., 2009a, *ApJ*, 706, 1163
 Livingstone M. A., Ransom S. M., Camilo F., Kaspi V. M., Lyne A. G., Kramer M., Stairs I. H., 2009b, *ApJ*, 706, 1163
 Lyne A. G., Graham-Smith F., 1990, *Pulsar astronomy*, Lyne A. G. & Graham-Smith F., ed. Cambridge: Cambridge Univ. Press
 Murray S. S., Slane P. O., Seward F. D., Ransom S. M., Gaensler B. M., 2002, *ApJ*, 568, 226
 Padrielli L. et al., 1986, *Astron. Astrophys.*, 165, 53
 Perley R. A., Fomalont E. B., Johnston K. J., 1980, *AJ*, 85, 649
 Ransom S. M., Demorest P., Ford J., McCullough R., Ray J., DuPlain R., Brandt P., 2009, in *American Astronomical Society Meeting Abstracts, Vol. 214, American Astronomical Society Meeting Abstracts #214*, p. #605.08
 Roberts D. A., Goss W. M., Kalberla P. M. W., Herbstmeier U., Schwarz U. J., 1993, *Astron. Astrophys.*, 274, 427
 Romney J. et al., 1984, *Astron. Astrophys.*, 135, 289
 Rudie G. C., Fesen R. A., 2007, in *Revista Mexicana de Astronomia y Astrofisica Conference Series, Vol. 30, Revista Mexicana de Astronomia y Astrofisica Conference Series*, pp. 90–95
 Schönrich R., 2012, *MNRAS*, 427, 274

- Shearer A., Neustroev V. V., 2008, MNRAS, 390, 235
Slane P., Helfand D. J., van der Swaluw E., Murray S. S.,
2004, ApJ, 616, 403
Slane P. O., Helfand D. J., Murray S. S., 2002, ApJL, 571,
L45
Stephenson F. R., Green D. A., 1999, Astronomy and Geo-
physics, 40, 27
van den Bergh S., 1990, ApJ, 357, 138
Weiler K. W., Panagia N., 1978, Astron. Astrophys., 70,
419